Journal of Hazardous Materials 184 (2010) 268–272

Contents lists available at ScienceDirect

Journal of Hazardous Materials

journal homepage: www.elsevier.com/locate/jhazmat

Immobilized redox mediator on metal-oxides nanoparticles and its catalytic effect in a reductive decolorization process

L.H. Alvarez [a], M.A. Perez-Cruz [b], J.R. Rangel-Mendez [a], F.J. Cervantes [a,*]

[a] División de Ciencias Ambientales, Instituto Potosino de Investigación Científica y Tecnológica (IPICyT), Camino a la Presa San José 2055, Col. Lomas 4a. Sección, 78216 San Luis Potosí, SLP, Mexico
[b] Facultad de Ciencias Químicas, Universidad Autónoma de Puebla, 72571 Puebla, Mexico

ARTICLE INFO

Article history:
Received 10 May 2010
Received in revised form 3 August 2010
Accepted 9 August 2010
Available online 17 August 2010

Keywords:
Quinones
Redox mediators
Immobilization
Nanoparticles

ABSTRACT

Different metal-oxides nanoparticles (MONP) including α-Al_2O_3, ZnO and $Al(OH)_3$, were utilized as adsorbents to immobilize anthraquinone-2,6-disulfonate (AQDS). Immobilized AQDS was subsequently tested as a solid-phase redox mediator (RMs) for the reductive decolorization of the azo dye, reactive red 2 (RR2), by anaerobic sludge. The highest adsorption capacity of AQDS was achieved on $Al(OH)_3$ nanoparticles, which was ~0.16 mmol g^{-1} at pH 4. Immobilized AQDS increased up to 7.5-fold the rate of decolorization of RR2 by anaerobic sludge as compared with sludge incubations lacking AQDS. Sterile controls including immobilized AQDS did not show significant (<3.5%) RR2 decolorization, suggesting that physical–chemical processes (*e.g.* adsorption or chemical reduction) were not responsible for the enhanced decolorization achieved. Immobilization of AQDS on MONP was very stable under the applied experimental conditions and spectrophotometric screening did not detect any detachment of AQDS during the reductive decolorization of RR2, confirming that immobilized AQDS served as an effective RMs. The present study constitutes the first demonstration that immobilized quinones on MONP can serve as effective RMs in the reductive decolorization of an azo dye. The immobilizing technique developed could be applied in anaerobic wastewater treatment systems to accelerate the redox biotransformation of recalcitrant pollutants.

1. Introduction

Several industrial sectors obtain great economical benefits due to the large and continuous production of different chemicals [1]. Nevertheless, linked to these economical benefits, several toxic and recalcitrant pollutants are discharged in large volumes of wastewater. Many of these contaminants are electron-accepting compounds, such as nitroaromatics, azo dyes, polyhalogenated compounds and metalloids, due to the presence of electrophilic functional groups in their structures, making difficult their treatment by convectional aerobic processes [2]. On the other hand, these pollutants can undergo reductive biotransformation under anaerobic conditions, producing compounds susceptible to aerobic biodegradation [3]. However, anaerobic reduction of recalcitrant pollutants occurs slowly as a result of toxicity effects on anaerobic consortia [4] or due to electron transfer limitations; consequently, anaerobic bioreactors could have deficient performance or can even collapse [5,6].

In the last years, humic substances (HS) and quinones (main redox reactive functional groups in HS) have been tested as redox mediators (RM) during the reductive biotransformation of electron-accepting priority pollutants [7–9]. RM decrease electron transfer limitations, so that biotransformation of these contaminants is accelerated, which minimizes the toxic effects in anaerobic microorganisms [4,6]. Nevertheless, water soluble RM, such as anthraquinone-2,6-disulfonate (AQDS), need to be continuously added to achieve increased reduction rates in anaerobic wastewater treatment processes; the continuous addition of RM increases the cost of treatment and generates contaminated effluents.

Few studies have shown the use of solid-phase RM (RMs) during the reductive biotransformation of priority pollutants. For instance, activated carbon was tested as a RMs due to the presence of quinone moieties in this material [10]. Moreover, quinoid RM has been immobilized in polymeric matrixes [11], on anion exchange resins [12], and on composites of polypyrrole [13]. In all these cases, the immobilized catalysts were shown to enhance the anaerobic biotransformation of azo dyes [10–12] or nitroaromatics [13].

Few years ago, with the emergence of nanotechnology, new materials have been designed and aimed to improve environmental quality through pollution prevention and treatment processes [14]. Mainly, nanoparticles are used as adsorbent materials of differ-

* Corresponding author. Tel.: +52 444 834 2041; fax: +52 444 834 2010.
E-mail address: fjcervantes@ipicyt.edu.mx (F.J. Cervantes).

0304-3894/$ – see front matter © 2010 Elsevier B.V. All rights reserved.
doi:10.1016/j.jhazmat.2010.08.032

ent organic and inorganic compounds for water treatment [14,15], including HS [16] and natural organic matter. Additionally, the adsorption of AQDS and HS has been conducted on ferrihydrite nanoparticles to evaluate the effect of adsorbed quinones on ferrihydrite reduction [17]. Furthermore, AQDS has also been adsorbed on hematite in order to understand geochemical variables during the reduction of iron oxides [18]. Nevertheless, to our knowledge, RM adsorbed on metal-oxides nanoparticles (MONP) have never been tested as RMs for the reductive biotransformation of priority pollutants, such as azo dyes. In this work, the capacity of different MONP to adsorb AQDS was evaluated. The catalytic properties of immobilized AQDS were subsequently tested in the reductive biotransformation of the azo model compound, reactive red 2 (RR2). RR2 is a very recalcitrant azo compound commonly used to represent reductive decolorization processes for textile wastewater treatment [6,12,19].

2. Experimental

2.1. Reagents and nanoparticles

AQDS (98% purity, Sigma Aldrich) was selected as a model RM. RR2 was purchased from Sigma Aldrich (purity of 40%) and used without further purification. Nanoparticles used for the immobilization of AQDS were the following metal-oxides: α-Al_2O_3, ZnO and $Al(OH)_3$. All nanoparticles have a purity ≥99%, and were purchased from Nanostructured & Amorphous Materials Inc. (Houston, TX, USA).

2.2. Inoculum

Anaerobic granular sludge was used as inoculum, and was collected from a full-scale upflow anaerobic sludge bed (UASB) reactor treating effluents from a malt-processing factory (Lara-Grajales, Puebla, Mexico). The sludge was previously acclimated in a lab-scale UASB reactor (1.5 L) operated at a hydraulic residence time of 12 h. Glucose was used as a sole energy source for the UASB reactor, which showed stable efficiencies in terms of chemical oxygen demand (COD) removal (>90%) during steady state conditions. Prior to incubations, stabilized sludge was washed with distilled water and disintegrated with sterile needles (Microlance 3, 25G5/8, 0.5 mm × 16 mm); in the same step, the sludge was stored in a glass serum bottle containing basal medium as describe in Section 2.4, and anaerobic conditions were established by saturating the inoculation bottle with a gas mixture of N_2/CO_2 (80%/20%).

2.3. Characterization of nanoparticles

Nanoparticles were characterized by nitrogen adsorption at 77 K, using a Physisorption equipment (Micromeritics ASAP 2020, Norcross, GA, USA) to calculate surface area (SA), applying the BET method. Before adsorption, samples were degassed at 383 K for 3 h. Pore volume (V_{P_0}) was calculated from the maximum adsorption amount of nitrogen at $p/p_0 = 0.99$ applying the Harkins and Jura method. Additionally, batch experiments were used to determinate the surface charge of all nanoparticles at different pH values under a CO_2-free atmosphere. N_2 was bubbled for 15 min into the solutions and also in the headspace of vials before sealing. First, 30 mg of nanoparticles were dispensed in vials, and portions of 0.1 M NaCl were used to keep a constant ionic strength. Initial pH values (3–11) were obtained by adding NaOH or HCl 0.1 M, for a total volume of 15 mL. After 7 days in stirring, the final pH was measured and the surface charge (expressed as the amount of ions released) was obtained with a mass balance based on pH change.

2.4. Immobilization of AQDS on nanoparticles

The capacity of MONP to immobilize AQDS was conducted by adsorption isotherms using the batch equilibrium technique. Different concentrations (50, 100, 200, 300, 400, 500 and 600 mg L^{-1}) of AQDS were prepared and the pH was adjust to 4.0 using 0.1 M HCl. Then, 50 mg of nanoparticles and 10 mL of AQDS solution were mixed in vials. Vials were placed on a shaker (180 rpm at 25 °C) until the equilibrium was accomplished. After centrifugation (5000 rpm, 10 min) the supernatant was analyzed in order to determine the equilibrium concentration of AQDS and the adsorption capacity.

The saturated materials were exposed several times to basal medium (pH 7.2) in order to verify the adsorption strength of AQDS on MONP. The basal medium was prepared according to the typical nutritional requirements for anaerobic wastewater treatment systems [4,6,10,12], which composition was as follows (mg L^{-1}): $NaHCO_3$ (3000), NH_4Cl (280), K_2HPO_4 (250), $MgSO_4.7H_2O$ (100), $CaCl_2.2H_2O$ (10), and 1 mL L^{-1} of trace element solution, which composition was as follows (mg L^{-1}): $FeCl_2{\cdot}4H_2O$ (2000), H_3BO_3 (50), $ZnCl_2$ (50), $CuCl_2{\cdot}2H_2O$ (38), $MnCl_2{\cdot}4H_2O$ (500), $(NH_4)6Mo_7O_{24}{\cdot}4H_2O$ (50), $AlCl_3{\cdot}6H_2O$ (90), $CoCl_2{\cdot}6H_2O$ (2000), $NiCl_2{\cdot}6H_2O$ (92), $Na_2SeO{\cdot}5H_2O$ (162), EDTA (1000), and 1 mL L^{-1} of HCl (36%). The produced materials were characterized by Fourier transform infrared (FTIR) spectrometry and were compared with the FTIR spectra of AQDS and nanoparticles, as mentioned in Section 2.6. In addition, energy dispersive X ray (EDX) analysis was determined as previously established [12].

2.5. Decolorization assays of RR2

Decolorization assays were performed in 120 mL serum glass bottles with the basal medium described above; $NaHCO_3$ was change to 5000 mg L^{-1} to create the proper buffer capacity (pH 7.2). Portions of basal medium, for a total volume of 50 mL, were dispensed in the bottles, which were then sealed with rubber stoppers and aluminum caps. The atmosphere in the headspace (70 mL) of the bottles was changed with a mixture of N_2/CO_2 (80%/20%) in order to create anaerobic conditions. Once the atmosphere was changed, the bottles were inoculated with anaerobic sludge (disintegrated) at 1 g of volatile suspended solids (VSS) per liter. All bottles were supplied with glucose (1 g COD L^{-1}) and pre-incubated during 12 h at 25 °C and 180 rpm. After the pre-incubation period, the bottles were flushed again with the same gas mixture and supplied with a second glucose pulse (2 g COD L^{-1}). RR2 was added from a stock solution prepared with sterile basal medium, and the initial concentration in the incubations was 0.3 mM. Different treatments and controls were tested in order to elucidate the catalytic effect of immobilized AQDS on nanoparticles. The treatments included three different concentrations (1.2, 2.4 and 4.8 mM) of AQDS in soluble and immobilized form. The controls were: first, a control without AQDS in any form, but including glucose, basal medium and sludge. Second, sterile controls with soluble or immobilized AQDS at 4.8 mM and basal medium. Finally, a control with nanoparticles, basal medium, sludge and glucose, but in the absence of AQDS. All conditions were carried out by triplicate and incubated at 25 °C and 180 rpm.

2.6. Analytical methods

AQDS concentration was spectrophotometrically measured at 328 nm. Liquid samples were firstly centrifuged (10 min at 10,000 rpm) and diluted in bicarbonate buffer (60 mM, pH 7.2). RR2 decolorization was also documented spectrophotometrically at the maximum wavelength of visible absorbance (539 nm). Samples (0.75 mL) were centrifuged and diluted in a 0.1 M phosphate buffer at pH 7.0. FTIR spectra were obtained at a resolution of

Table 1
Characterization and adsorption capacity of AQDS on the different nanoparticles tested.

Nanoparticle	D_P[a] (nm)	SA[b] ($m^2\ g^{-1}$)	V_{P_0}[c] ($cm^3\ g^{-1}$)	pH_{PZC}[d]	Q_{des}[e] (mmol g^{-1})
α-Al_2O_3-1	35	10.05	0.018	7.9	7.03×10^{-3}
α-Al_2O_3-2	150	8.89	0.015	7.9	1.56×10^{-3}
ZnO	20	37.97	0.159	7.5	6.31×10^{-3}
$Al(OH)_3$	15	62.40	0.138	4.8	1.05×10^{-1}

[a] Particle diameter.
[b] Surface area.
[c] Porous volume.
[d] pH of zero point charge.
[e] Adsorption capacity after various desorption cycles in basal medium.

4 cm^{-1} using a FTIR spectrometer (Thermo Scientific, Nicolet 6700) equipped with an attenuated total reflection (ATR) accessory. Samples were previously dried at 40 °C in an oven.

3. Results and discussion

3.1. Characterization of nanoparticles

Characterization of the evaluated MONP is summarized in Table 1. The highest particle diameter (D_P) corresponds to α-Al_2O_3-2, while the smallest D_P value was found for $Al(OH)_3$. SA of nanoparticles follows the order: $Al(OH)_3$ > ZnO > α-Al_2O_3-1 > α-Al_2O_3-2. Regarding V_{P_0} data, nanoparticles showed different values from 0.018 to 0.159 $cm^3\ g^{-1}$. There is a relationship between the V_{P_0} and SA values, but an indirect relationship between SA and D_P values (*e.g.* the small SA found in α-Al_2O_3-2 (8.89 $m^2\ g^{-1}$) is attributed to its relatively large D_P and small V_{P_0} value).

Surface charge data at different pH values are given in Fig. 1. Surface charge of all MONP decreased with the increase of pH. Both, α-Al_2O_3-1 and α-Al_2O_3-2 had positive charges on their surfaces below its pH point of zero charge (pH_{PZC}), and negative charges over its pH_{PZC}; the pH_{PZC} of these nanoparticles was 7.9. The highest surface charge at pH 3.0 corresponds to $Al(OH)_3$, but relatively low surface charge values were observed at the pH range between 5 and 11. Finally, the pH_{PZC} identified for ZnO nanoparticles was 7.5.

3.2. Adsorption of AQDS on nanoparticles

Adsorption isotherms of AQDS on nanoparticles are presented in Fig. 2. The highest adsorption capacity was achieved on $Al(OH)_3$ nanoparticles, while similar adsorption capacity was observed for the two types of α-Al_2O_3 and ZnO. The isotherm with $Al(OH)_3$ showed an initial slope for the lower concentrations of AQDS tested, then a plateau and maximum adsorption capacity was observed (~0.16 mmol g^{-1}). AQDS adsorption on $Al(OH)_3$ is pH dependent (Fig. 2); a lower adsorption capacity was achieved at pH 7.0 compared to that obtained at pH 4.0, with values of 0.099 and 0.168 mmol g^{-1}, respectively. The adsorption of AQDS on the two types of α-Al_2O_3 and on ZnO was similar and within the range of 8.4×10^{-2} to 1.2×10^{-2} mmol g^{-1}; one order of magnitude lower than the adsorption capacity accomplished with $Al(OH)_3$. The adsorption capacity of $Al(OH)_3$ is much higher than that achieved with previously tested materials such as hematite, α-alumina and ferrihydrite [17,18], which immobilized AQDS for different purposes to that aimed in the present study. The adsorption capacity of $Al(OH)_3$ is also higher than that obtained during the immobilization of AQDS on an anion exchange resin, which was subsequently shown to effectively increase the reductive decolorization of several azo dyes by serving as a RMs [12].

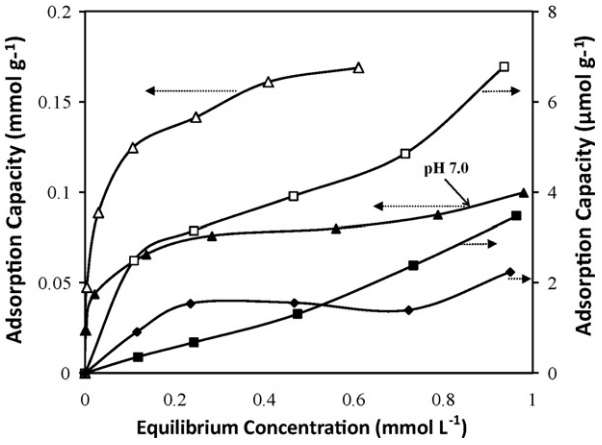

Fig. 2. Adsorption capacity of AQDS on MONP at pH 4; the initials AQDS concentrations were 50–600 mg L^{-1}. Symbols: (■) α-Al_2O_3-1, (□) α-Al_2O_3-2, (♦) ZnO, (△) $Al(OH)_3$ and (▲) $Al(OH)_3$ at pH 7.0.

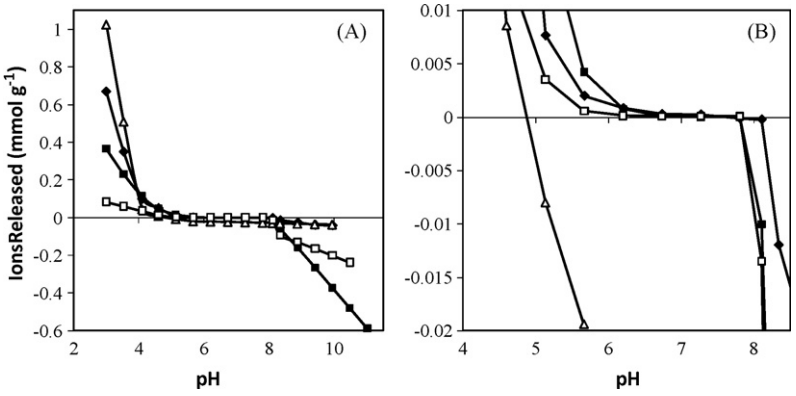

Fig. 1. Surface charge of MONP using NaCl 0.1 mM to maintain a constant ionic strength. (A) Surface charge considering all pH values tested. (B) Approach of panel A to identify the pH_{PZC} of MONP. Symbols: (■) α-Al_2O_3-1, (□) α-Al_2O_3-2, (♦) ZnO and (△) $Al(OH)_3$.

Table 2
First-order rate constant of decolorization (k_d) of reactive red 2 using immobilized redox mediators and anaerobic sludge[a].

Condition	RM concentration (mM)	k_d (d^{-1})	Increase in k_d[b]	Decolorization efficiency (%)
AQDS-im[c]	1.2	0.71 ± 0.01	4.77 ± 0.11	30.1 ± 0.60
	2.4	0.83 ± 0.05	5.57 ± 0.47	34.2 ± 1.65
	4.8	1.13 ± 0.01	7.52 ± 0.10	43.2 ± 0.43
AQDS-so[d]	1.2	3.47 ± 0.27	23.11 ± 1.81	81.2 ± 2.55
	2.4	3.31 ± 0.14	22.04 ± 0.97	80.9 ± 1.43
	4.8	3.41 ± 0.14	22.68 ± 0.95	81.8 ± 1.31

[a] Conditions: glucose concentration, 2 g COD/L; sludge concentration (disintegrated), 1 g VSS/L; RR2 concentration, 0.3 mM.
[b] Increase observed on k_d with respect to the control lacking AQDS (k_d in quinone-amended cultures/k_d in control), which was 0.151 d^{-1}. Data represent average of triplicate determinations ± standard deviation.
[c] AQDS immobilized on $Al(OH)_3$ nanoparticles.
[d] Refers to quinones, which were not immobilized, but provided in soluble form.

According to the surface charge values (Fig. 1), AQDS adsorption could be attributed to electrostatic interaction between positive charges of the nanoparticles at pH 4.0, and negative charges of ionized sulfonate groups (SO_3^-) of AQDS, similar to the interaction of AQDS with hematite [18]. Nevertheless, it could be possible that an additional mechanism, such as affinity, might be involved for AQDS adsorption on $Al(OH)_3$; this is implied by the superior adsorption capacity observed with this material even though its surface charge, at the pH at which adsorption took place (4.0), is lower than that found on α-Al_2O_3-1, and ZnO (Fig. 2).

In order to verify the strength at which AQDS was immobilized on the different MONP evaluated, the saturated materials were exposed to four desorption cycles with a basal medium, which resembles the typical nutritional conditions prevailing in anaerobic wastewater treatment systems. All saturated MONP showed desorption of AQDS during the first desorption cycle, probably due to detachment of quinones not electrostatically interacting with MONP, but forming multi-layers during the adsorption process. The amount of AQDS desorbed after the desorption cycles, was (%): $Al(OH)_3$ (37.8), ZnO (32.1), α-Al_2O_3-1 (16.8) and α-Al_2O_3-2 (85.8). Immobilized AQDS remained stable after this washing procedure and throughout its application during the reductive decolorization of RR2 (see below). The adsorption capacities of AQDS on MONP after desorption cycles are listed in Table 1.

EDX analysis confirmed adsorption of AQDS on nanoparticles of $Al(OH)_3$ as an increase in the content of C and S was detected in the surface of AQDS-amended $Al(OH)_3$ nanoparticles, compared with their counterpart lacking this quinoid RM; whereas a decrease in the content of Al and O occurred once AQDS was adsorbed on this material (Table S1, Supplementary data). Finally, FTIR spectra revealed that carbonyl groups of AQDS, which are the redox mediating groups of this catalyst, remained available once adsorbed on $Al(OH)_3$ (SD, Supplementary data, Fig. S1). Certainly, the characteristic spectral signal of both carbonyl (C=O) and sulfonate (SO_3^-) groups at 1700–1630 cm^{-1} and 1200–1100 cm^{-1}, respectively, were detected in FTIR spectra of AQDS-amended $Al(OH)_3$ nanoparticles. These functional groups were also detected in the spectra of AQDS, but not in $Al(OH)_3$ nanoparticles lacking AQDS.

3.3. Decolorization of RR2 with immobilized AQDS

Nanoparticles of $Al(OH)_3$ were selected as immobilizing material of AQDS to verify if the synthesized composite could efficiently increase the reductive decolorization of the azo model compound RR2 by serving as RMs in sludge incubations. Decolorization of RR2 followed first-order kinetics and the first-order rate constants of decolorization were calculated according to the following equation:

$$A = A_o e^{-kdt}$$

where A is absorbance at a given time; A_o is the initial absorbance; k_d is the first-order rate constant of decolorization and t is time.

Typical decolorization profiles are shown in SD (Supplementary data, Fig. S2). Sterile controls provided with the highest concentration of AQDS tested (4.8 mM), either immobilized (AQDS-im) or soluble (AQDS-so), did not show significant (<3.5%) decolorization of RR2 indicating that physical–chemical processes (*e.g.* adsorption or chemical reduction) were not responsible for the reductive decolorization of RR2 achieved in sludge incubations. Controls including biologically active sludge incubated without AQDS achieved only 7.2% of RR2 decolorization. The catalytic effect of AQDS-im could be confirmed by the increased k_d values achieved during the reductive decolorization of RR2 by anaerobic sludge when the immobilized RM was included in sludge incubations (Table 2). The rate of decolorization of RR2 was increased up to 7.5-fold in the presence of AQDS-im as compared with the biologically active control lacking AQDS. The catalytic effect of AQDS-im was also favorably reflected in a greater extent of decolorization of RR2. Indeed, up to 43.2% of RR2 decolorization occurred in sludge incubations supplied with AQDS-im after 12 h of incubation, whereas only 7.2% of RR2 decolorization was achieved in sludge incubation without AQDS during the same incubation period. Spectrophotometric screening (SD, Supplementary data, Fig. S3) performed during the decolorization of RR2 (and even after 5 days of incubation) in the presence of AQDS-im did not detect any detachment of AQDS confirming that the enhanced decolorization achieved could exclusively be attributed to the redox mediating capacity of the immobilized catalyst.

Previous studies reported different approaches to apply RMs during the redox biotransformation of azo dyes [10–12,20] and nitroaromatics [13]. Some disadvantages of these immobilizing techniques are the gradual loss of the redox mediating capacity due to either wash-out of the RMs from bioreactors [10] or disruption of the immobilizing material [11] and mass transfer limitations because a major fraction of the RMs remained entrapped within the immobilizing material [11]. To our knowledge the present study constitute the first demonstration that quinoid RM immobilized in MONP can serve as an effective RMs in a reductive decolorization process.

A series of experiments with AQDS-so was also conducted in order to compare with the results derived from sludge incubations provided with AQDS-im. As expected, the rates of decolorization achieved in incubations amended with AQDS-so were higher than those achieved with AQDS-im. AQDS-so increased up to 23.1-fold the decolorization rate of RR2 as compared with the control lacking AQDS, which allowed decolorization efficiencies of up 81.8% after 12 h of incubation. Despite the lower decolorization rates achieved with AQDS-im as compared with those obtained with AQDS-so, there are several advantages for considering MONP as immobilizing material of RM. Firstly, MONP can economically be synthesized. Secondly, MONP have a larger capacity to immobilize quinoid RM or HS compared to other materials [17,18]. Moreover, MONP have the proper physical–chemical properties to prevent disruption of the immobilized catalysts. Furthermore, mass transfer limitations

occurring with other immobilizing materials could be overcome by using MONP to immobilize RM. Certainly, AQDS immobilized on an anion exchange resin and tested as a RMs, under the same experimental conditions applied in the present study, increased the rate of the decolorization of RR2 only by ~2-fold [12], whereas an enhancement of up to 7.5-fold was achieved in the present study by using nanoparticles of $Al(OH)_3$ as immobilizing material. The redox mediating capacity of AQDS immobilized in MONP is also superior to other RMs immobilized by different approaches [11,13], which also have mass transfer limitations. Further experiments in our group have revealed that MONP can also serve as an effective matrix to immobilize HS and this immobilized material efficiently increase the redox biotransformation of different electron-accepting pollutants, such as azo dyes and carbon tetrachloride.

Perminova et al. [21] developed a procedure to covalently bind HS to alumina particles by alkoxysilylation and this material was shown to efficiently remove Np(V) and Pu(V) by the sequestering properties of the immobilized HS [22]. However, this immobilized material has not been tested in redox reactions yet, but seems to fulfill the requirements to serve as a RMs feasible for remediation purposes.

Finally, although the catalytic effect of AQDS-im was demonstrated in the present study, the use of MONP in anaerobic wastewater treatment systems requires some important considerations in order to prevent their wash-out. An alternative to warrant the maintenance of this RMs in anaerobic bioreactors is by creating granules in which HS-amended MONP and anaerobic sludge are simultaneously immobilized. This will be the subject of an upcoming research.

4. Conclusions

Immobilized AQDS on nanoparticles of $Al(OH)_3$ could serve as an effective RMs during the reductive decolorization of RR2 by an anaerobic sludge. Compared with the control lacking quinones, incubations with AQDS-im increased up to 7.5-fold the rate of decolorization of RR2. Spectrophotometric screening did not detect any detachment of AQDS during the reductive decolorization of RR2, indicating that the enhanced decolorization achieved could be exclusively attributed to the immobilized catalyst. Mass transfer limitations could be decreased by using nanoparticles to immobilize RM in comparison with other materials previously explored.

Acknowledgements

This study was financially supported by the Lettinga Associates Foundation (Lettinga Award 2007) and by the Council of Science and Technology of Mexico (Grant SEP-CONACYT 55045). M.A. Perez-Cruz acknowledges to CONACYT for the scholarship to support postdoctoral position. Also, the authors appreciate the technical assistance of Dulce Partida Gutiérrez, Hugo Hernández Gutiérrez and Guillermo Vidriales Escobar. Characterization of nanoparticles was carried out at Laboratorio Nacional de Biotecnología Agrícola, Médica y Ambiental (LANBAMA, IPICYT).

Appendix A. Supplementary data

Supplementary data associated with this article can be found, in the online version, at doi:10.1016/j.jhazmat.2010.08.032.

References

[1] E. Razo-Flores, H. Macarie, F. Morier, Application of biological treatment systems for chemical and petrochemical wastewaters, in: F.J. Cervantes, S.G. Pavlostathis, A.C. Van Haandel (Eds.), Advanced Biological Treatment Processes for Industrial Wastewaters: Principles & Applications, IWA Publishing, London, UK, 2006, pp. 267–297.
[2] F.P. Van der Zee, F.J. Cervantes, Impact and application of electron shuttles on the redox (bio)transformation of contaminants: a review, Biotechnol. Adv. 27 (2009) 256–277.
[3] J.A. Field, A.J.M. Stams, M. Kato, G. Schraa, Enhanced biodegradation of aromatic pollutants in cocultures of anaerobic and aerobic bacterial consortia, Anton. Leeuw. Int. J. G. 67 (1995) 47–77.
[4] F.J. Cervantes, M.I. López-Vizcarra, E. Siqueiros, E. Razo-Flores, Riboflavin prevents inhibitory effects during the reductive decolorization of Reactive Orange 14 by methanogenic sludge, J. Chem. Technol. Biotechnol. 83 (2008) 1703–1709.
[5] J.D. Rodgers, N.J. Bunce, Treatment methods for the remediation of nitroaromatic explosives, Water Res. 35 (2001) 2101–2111.
[6] F.P. Van der Zee, R.H.M. Bouwman, D.P.B.T.B. Strik, G. Lettinga, J.A. Field, Application of redox mediators to accelerate the transformation of reactive azo dyes in anaerobic bioreactors, Biotechnol. Bioeng. 75 (2001) 691–701.
[7] J. Rau, H.J. Knackmuss, A. Stolz, Effects of different quinoid redox mediators on the anaerobic reduction of azo dyes by bacteria, Environ. Sci. Technol. 36 (2002) 1497–1504.
[8] T. Borch, W.P. Inskeep, J.A. Harwood, R. Gerlach, Impact of ferrihydrite and anthraquinone-2,6-disulfonate on the reductive transformation of 2,4,6-trinitrotoluene by a Grampositive fermenting bacterium, Environ. Sci. Technol. 39 (2005) 7126–7133.
[9] A.L. Barkovskii, P. Adriaens, Impact of humic constituents on microbial dechlorination of polychlorinated dioxins, Environ. Toxicol. Chem. 17 (1998) 1013–1020.
[10] F.P. Van der Zee, I.A. Bisschops, G. Lettinga, J.A. Field, Activated carbon as an electron acceptor and redox mediator during the anaerobic biotransformation of azo dyes, Environ. Sci. Technol. 37 (2003) 402–408.
[11] J. Guo, J. Zhou, D. Wang, C. Tian, P. Wang, M.S. Uddin, H. Yu, Biocalalyst effects of immobilized anthraquinone on the anaerobic reduction of azo dyes by the salttolerant bacteria, Water Res. 41 (2007) 426–432.
[12] F.J. Cervantes, A. Garcia-Espinosa, M.A. Moreno-Reynosa, J.J. Rangel-Mendez, Immobilized redox mediators on anion exchange resins and their role on the reductive decolorization of azo dyes, Environ. Sci. Technol. 44 (2010) 1747–1753.
[13] L. Li, J. Wang, J. Zhou, F. Yang, C. Jin, Y. Qu, A. Li, L. Zhang, Enhancement of nitroaromatic compounds anaerobic biotransformation using a novel immobilized redox mediator prepared by electropolymerization, Bioresour. Technol. 99 (2008) 6908–6916.
[14] T. Masciangioli, Z. Wei-Xian, Environmental technologies at the nanoscale, Environ. Sci. Technol. 37 (2003) 102A–108A.
[15] J. Theron, J.A. Walker, T.E. Cloete, Nanotechnology and water treatment: applications and emerging opportunities, Crit. Rev. Microbiol. 34 (2008) 43–69.
[16] K. Yang, D. Lin, B. Xing, Interactions of humic acid with nanosized inorganic oxides, Langmuir 25 (2009) 3571–3576.
[17] M. Wolf, A. Kappler, J. Jiang, R. Meckenstock, Effects of humic substances and quinones at low concentrations on ferrihydrite reduction by geobacter metallireducens, Environ. Sci. Technol. 43 (2009) 5679–5685.
[18] C. Liu, J.M. Zachara, N.S. Foster, J. Strickland, Kinetics of reductive dissolution of hematite by bioreduced anthraquinone-2,6-disulfonate, Environ. Sci. Technol. 41 (2007) 7730–7735.
[19] S.G. Pavlostathis, M.I. Beydilli, Decolorization kinetics of the azo dye reactive red 2 under methanogenic conditions: effect of long-term culture acclimation, Biodegradation 16 (2005) 135–146.
[20] G. Mezohegyi, A.U. Kolodkin, I. Castro, C. Bengoa, F. Stuber, J. Font, A. Fabregat, Effective anaerobic decolorization of azo dye Acid Orange 7 in continuous upflow packed-bed reactor using biological activated carbon system, Ind. Eng. Chem. Res. 46 (2007) 6788–6792.
[21] I. Perminova, S. Ponomarenko, L. Karpiouk, K. Hatfield, PCT application RU2006/000102, Humic derivatives, methods of preparation and use, Filed on March 7, 2006.
[22] I. Perminova, L. Karpiouk, N. Shcherbina, S. Ponomarenko, S. Kalmykov, K. Hatfield, Preparation and use of humic coatings covalently bound to silica gel for Np(V) and Pu(V) sequestration, J. Alloy Compd. 444–445 (2007) 512–517.